

World Journal of *Gastroenterology*

World J Gastroenterol 2024 January 28; 30(4): 286-423



EDITORIAL

- 286** Revolutionizing gastric cancer treatment: The potential of immunotherapy
Christodoulidis G, Koumarelas KE, Kouliou MN

REVIEW

- 290** Portal hypertension in patients with nonalcoholic fatty liver disease: Current knowledge and challenges
Madir A, Grgurevic I, Tsouchatzis EA, Pinzani M

ORIGINAL ARTICLE**Retrospective Study**

- 308** Value of multiple models of diffusion-weighted imaging to predict hepatic lymph node metastases in colorectal liver metastases patients
Zhu HB, Zhao B, Li XT, Zhang XY, Yao Q, Sun YS

- 318** Hepatic arterial infusion chemotherapy with anti-angiogenesis agents and immune checkpoint inhibitors for unresectable hepatocellular carcinoma and meta-analysis
Cao YZ, Zheng GL, Zhang TQ, Shao HY, Pan JY, Huang ZL, Zuo MX

Observational Study

- 332** Circulating microRNA expression and nonalcoholic fatty liver disease in adolescents with severe obesity
Li YJ, Baumert BO, Stratakis N, Goodrich JA, Wu HT, He JX, Zhao YQ, Aung MT, Wang HX, Eckel SP, Walker DI, Valvi D, La Merrill MA, Ryder JR, Inge TH, Jenkins T, Sisley S, Kohli R, Xanthakos SA, Baccarelli AA, McConnell R, Conti DV, Chatzi L
- 346** Gastrointestinal manifestations of critical ill heatstroke patients and their associations with outcomes: A multicentre, retrospective, observational study
Wang YC, Jin XY, Lei Z, Liu XJ, Liu Y, Zhang BG, Gong J, Wang LT, Shi LY, Wan DY, Fu X, Wang LP, Ma AJ, Cheng YS, Yang J, He M, Jin XD, Kang Y, Wang B, Zhang ZW, Wu Q

Basic Study

- 367** Amlodipine inhibits the proliferation and migration of esophageal carcinoma cells through the induction of endoplasmic reticulum stress
Chen YM, Yang WQ, Gu CW, Fan YY, Liu YZ, Zhao BS

SYSTEMATIC REVIEWS

- 381** Current status of magnetic resonance imaging radiomics in hepatocellular carcinoma: A quantitative review with Radiomics Quality Score
Brancato V, Cerrone M, Garbino N, Salvatore M, Cavalieri C

LETTER TO THE EDITOR

- 418** Antiviral treatment standards for hepatitis B: An urgent need for expansion

Bao ZH, Dai ZK, Tang HX

- 421** Leukocyte immunoglobulin-like receptor B2: A promising biomarker for colorectal cancer

Zhao WZ, Wang HG, Yang XZ

Contents

ABOUT COVER

Editorial Board Member of *World Journal of Gastroenterology*, Giuseppe Sica, MD, PhD, Professor of Surgery, Department of Surgical Science, Tor Vergata University Hospital, Rome 00133, Italy. giuseppe.sica@ptvonline.it

AIMS AND SCOPE

The primary aim of *World Journal of Gastroenterology* (WJG, *World J Gastroenterol*) is to provide scholars and readers from various fields of gastroenterology and hepatology with a platform to publish high-quality basic and clinical research articles and communicate their research findings online. WJG mainly publishes articles reporting research results and findings obtained in the field of gastroenterology and hepatology and covering a wide range of topics including gastroenterology, hepatology, gastrointestinal endoscopy, gastrointestinal surgery, gastrointestinal oncology, and pediatric gastroenterology.

INDEXING/ABSTRACTING

The WJG is now abstracted and indexed in Science Citation Index Expanded (SCIE), MEDLINE, PubMed, PubMed Central, Scopus, Reference Citation Analysis, China Science and Technology Journal Database, and Superstar Journals Database. The 2023 edition of Journal Citation Reports® cites the 2022 impact factor (IF) for WJG as 4.3; Quartile category: Q2. The WJG's CiteScore for 2021 is 8.3.

RESPONSIBLE EDITORS FOR THIS ISSUE

Production Editor: Yu-Xi Chen; Production Department Director: Xiang Li; Editorial Office Director: Jia-Ru Fan.

NAME OF JOURNAL

World Journal of Gastroenterology

ISSN

ISSN 1007-9327 (print) ISSN 2219-2840 (online)

LAUNCH DATE

October 1, 1995

FREQUENCY

Weekly

EDITORS-IN-CHEIF

Andrzej S Tarnawski

EXECUTIVE ASSOCIATE EDITORS-IN-CHEIF

Xian-Jun Yu (Pancreatic Oncology), Jian-Gao Fan (Chronic Liver Disease), Hou-Bao Liu (Biliary Tract Disease)

EDITORIAL BOARD MEMBERS

<http://www.wjgnet.com/1007-9327/editorialboard.htm>

PUBLICATION DATE

January 28, 2024

COPYRIGHT

© 2024 Baishideng Publishing Group Inc

PUBLISHING PARTNER

Shanghai Pancreatic Cancer Institute and Pancreatic Cancer Institute, Fudan University
Biliary Tract Disease Institute, Fudan University

INSTRUCTIONS TO AUTHORS

<https://www.wjgnet.com/bpg/gerinfo/204>

GUIDELINES FOR ETHICS DOCUMENTS

<https://www.wjgnet.com/bpg/GerInfo/287>

GUIDELINES FOR NON-NATIVE SPEAKERS OF ENGLISH

<https://www.wjgnet.com/bpg/gerinfo/240>

PUBLICATION ETHICS

<https://www.wjgnet.com/bpg/GerInfo/288>

PUBLICATION MISCONDUCT

<https://www.wjgnet.com/bpg/gerinfo/208>

POLICY OF CO-AUTHORS

<https://www.wjgnet.com/bpg/GerInfo/310>

ARTICLE PROCESSING CHARGE

<https://www.wjgnet.com/bpg/gerinfo/242>

STEPS FOR SUBMITTING MANUSCRIPTS

<https://www.wjgnet.com/bpg/GerInfo/239>

ONLINE SUBMISSION

<https://www.f6publishing.com>

PUBLISHING PARTNER'S OFFICIAL WEBSITE

<https://www.shca.org.cn>
<https://www.zs-hospital.sh.cn>

Submit a Manuscript: <https://www.f6publishing.com>*World J Gastroenterol* 2024 January 28; 30(4): 308-317

DOI: 10.3748/wjg.v30.i4.308

ISSN 1007-9327 (print) ISSN 2219-2840 (online)

ORIGINAL ARTICLE

Retrospective Study

Value of multiple models of diffusion-weighted imaging to predict hepatic lymph node metastases in colorectal liver metastases patients

Hai-Bin Zhu, Bo Zhao, Xiao-Ting Li, Xiao-Yan Zhang, Qian Yao, Ying-Shi Sun

Specialty type: Gastroenterology and hepatology**Provenance and peer review:**

Unsolicited article; Externally peer reviewed.

Peer-review model: Single blind**Peer-review report's scientific quality classification**

Grade A (Excellent): 0

Grade B (Very good): B, B

Grade C (Good): 0

Grade D (Fair): 0

Grade E (Poor): 0

P-Reviewer: Koehler H, Germany; Padilla M, Latvia**Received:** November 6, 2023**Peer-review started:** November 6, 2023**First decision:** November 30, 2023**Revised:** December 15, 2023**Accepted:** January 10, 2024**Article in press:** January 10, 2024**Published online:** January 28, 2024**Hai-Bin Zhu, Bo Zhao, Xiao-Ting Li, Xiao-Yan Zhang, Ying-Shi Sun**, Key Laboratory of Carcinogenesis and Translational Research (Ministry of Education/Beijing), Department of Radiology, Peking University Cancer Hospital and Institute, Beijing 100142, China**Qian Yao**, Key Laboratory of Carcinogenesis and Translational Research (Ministry of Education/Beijing), Department of Pathology, Peking University Cancer Hospital and Institute, Beijing 100142, China**Corresponding author:** Ying-Shi Sun, MD, Chief Physician, Professor, Key Laboratory of Carcinogenesis and Translational Research (Ministry of Education/Beijing), Department of Radiology, Peking University Cancer Hospital and Institute, No. 52 Fucheng Road, Haidian District, Beijing 100142, China. sys27@163.com

Abstract

BACKGROUND

About 10%-31% of colorectal liver metastases (CRLM) patients would concomitantly show hepatic lymph node metastases (LNM), which was considered as sign of poor biological behavior and a relative contraindication for liver resection. Up to now, there's still lack of reliable preoperative methods to assess the status of hepatic lymph nodes in patients with CRLM, except for pathology examination of lymph node after resection.

AIM

To compare the ability of mono-exponential, bi-exponential, and stretched-exponential diffusion-weighted imaging (DWI) models in distinguishing between benign and malignant hepatic lymph nodes in patients with CRLM who received neoadjuvant chemotherapy prior to surgery.

METHODS

In this retrospective study, 97 CRLM patients with pathologically confirmed hepatic lymph node status underwent magnetic resonance imaging, including DWI with ten b values before and after chemotherapy. Various parameters, such as the apparent diffusion coefficient from the mono-exponential model, and the true diffusion coefficient, the pseudo-diffusion coefficient, and the perfusion fraction derived from the intravoxel incoherent motion model, along with distributed diffusion coefficient (DDC) and α from the stretched-exponential

model (SEM), were measured. The parameters before and after chemotherapy were compared between positive and negative hepatic lymph node groups. A nomogram was constructed to predict the hepatic lymph node status. The reliability and agreement of the measurements were assessed using the coefficient of variation and intraclass correlation coefficient.

RESULTS

Multivariate analysis revealed that the pre-treatment DDC value and the short diameter of the largest lymph node after treatment were independent predictors of metastatic hepatic lymph nodes. A nomogram combining these two factors demonstrated excellent performance in distinguishing between benign and malignant lymph nodes in CRLM patients, with an area under the curve of 0.873. Furthermore, parameters from SEM showed substantial repeatability.

CONCLUSION

The developed nomogram, incorporating the pre-treatment DDC and the short axis of the largest lymph node, can be used to predict the presence of hepatic LNM in CRLM patients undergoing chemotherapy before surgery. This nomogram was proven to be more valuable, exhibiting superior diagnostic performance compared to quantitative parameters derived from multiple b values of DWI. The nomogram can serve as a preoperative assessment tool for determining the status of hepatic lymph nodes and aiding in the decision-making process for surgical treatment in CRLM patients.

Key Words: Colorectal cancer; Individualized treatment; Diffusion magnetic resonance imaging; Intravoxel incoherent motion; Liver

©The Author(s) 2024. Published by Baishideng Publishing Group Inc. All rights reserved.

Core Tip: This study compared the diagnostic effectiveness of mono-exponential, bi-exponential, and stretched exponential Diffusion-weighted magnetic resonance imaging in predicting hepatic lymph node metastases (LNM) in patients with colorectal liver metastases after chemotherapy. Our finding indicated that only the pre-treatment distributed diffusion coefficient value and the short diameter of the largest lymph node after treatment were independent predictors of hepatic LNM. We developed a nomogram incorporating these two factors to non-invasively and individually predict the status of hepatic lymph nodes, demonstrating significant potential in surgical planning and assessing high-risk patients.

Citation: Zhu HB, Zhao B, Li XT, Zhang XY, Yao Q, Sun YS. Value of multiple models of diffusion-weighted imaging to predict hepatic lymph node metastases in colorectal liver metastases patients. *World J Gastroenterol* 2024; 30(4): 308-317

URL: <https://www.wjgnet.com/1007-9327/full/v30/i4/308.htm>

DOI: <https://dx.doi.org/10.3748/wjg.v30.i4.308>

INTRODUCTION

Colorectal carcinoma ranks as the most prevalent digestive tumors globally, with over 50% of patients developing colorectal liver metastases (CRLM) either at diagnosis (synchronous metastases) or during follow-up (metachronous metastases)[1]. Currently, the preferred approach in standard treatment guidelines involves perioperative chemotherapy combined with surgical resection, particularly when achieving complete resection with sufficient residual liver parenchyma is feasible[2,3]. Approximately 10%-31% of CRLM patients exhibit hepatic lymph node metastases (LNM), representing an adverse prognostic factor with significant impact on outcomes[4,5]. Surgery remains the sole potentially curative therapy if LNM are confined to the hepatic pedicle, although this procedure may be associated with potential postoperative complications, such as bleeding, lymphatic leakage, and ischemic bile duct stricture[6,7].

The gold standard for evaluating LNM still relies on histopathological assessment post-operation. Currently, there is inconsistency in the indications for lymphadenectomy in CRLM, partly due to the challenge of preoperatively predicting LNM. For instance, Grobmyer *et al*[8] examined 100 patients with hepatic lymph nodes undergoing resection for primary and metastatic hepatic malignancies. They found that both CT and intraoperative clinical palpation had a high negative predictive value (NPV = 95% and 99%, respectively) with a low positive predictive value (PPV = 30% and 39%, respectively). Similarly, Rau *et al*[9] discovered that a short diameter of lymph nodes larger than 15 mm and a morphologically round shape on computed tomography (CT) had a high NPV of 85% but a relatively low PPV of 43% for LNM. Intriguingly, up to 27% of patients with confirmed pathological LNM were not initially suspected using a combination of CT and intraoperative examination. Therefore, there is a crucial need for reliable predictors of LNM in CRLM before surgery to precisely guide individual decision-making and prevent overtreatment in low-risk patients.

Diffusion-weighted imaging (DWI) has undergone extensive investigation for its utility in cancer detection, treatment response assessment, and prognosis evaluation[10-12]. The apparent diffusion coefficient (ADC), derived from DWI,

exhibits promising capabilities in distinguishing lymph nodes, providing a noninvasive assessment of the microscopic random Brownian motion of water molecules in biological tissues. For instance, Sumi *et al*[13] observed higher ADC values in metastatic lymph nodes compared to benign non-metastatic lymph nodes, whereas Abdel Razek *et al*[14] and Eiber *et al*[15] reported lower ADC values in metastatic lymph nodes. This inconsistency may arise from the mono-exponential decay formula used to calculate ADC values, assuming tissue homogeneity and water molecule movement with a Gaussian distribution. Intravoxel incoherent motion (IVIM) is a technique capable of potentially differentiating perfusion components from the pure diffusion of water molecules using a biexponential model. This model allows for the quantification of three parameters: The true diffusion coefficient (D), the pseudo-diffusion coefficient (D^*), and the perfusion fraction (f). Consequently, parameters obtained from the IVIM model have demonstrated superior diagnostic performance compared to traditional ADC in differentiating hepatic lesions in previous studies[16,17]. More recently, Bennett *et al*[18] introduced the stretched-exponential model (SEM), providing an alternative approach to quantify intravoxel heterogeneity. The SEM employs two parameters: The distributed diffusion coefficient (DDC) and the intravoxel water diffusion heterogeneity (α). However, to date, there remains a paucity of studies comparing functional magnetic resonance imaging (MRI) parameters derived from different models to determine the status of hepatic lymph nodes in CRLM patients.

The objective of this study was to assess the diagnostic accuracy of three mathematical models of DWI in distinguishing between benign and malignant hepatic lymph nodes in CRLM patients who underwent chemotherapy prior to surgery.

MATERIALS AND METHODS

Study participants

This retrospective study protocol received approval from the Medical Ethics Committee of Beijing Cancer Hospital, and informed consent was waived.

CRLM patients with a pathologic diagnosis of hepatic lymph nodes in our hospital between January 2015 and January 2023 were included in this study. Patients had to undergo at least two cycles of neoadjuvant chemotherapy and undergo MRI examinations before neoadjuvant chemotherapy (pre-treatment point) and within 1 mo before surgery (post-treatment point). Exclusion criteria were: (1) Patients who underwent hepatectomy without hepatic lymph node resection; (2) Patients without measurable hepatic lymph nodes > 5 mm on the baseline MRI; and (3) Patients without multiple b-values of DWI sequence or insufficient quality of DWI for analysis. A total of 97 patients were enrolled in this study.

MRI protocol

All patients underwent MRI examinations using a 1.5T MRI device (Signa Excite II; GE Healthcare, Milwaukee, WI, United States) equipped with an 8-channel phased array body coil. The imaging protocol included axial T2-weighted imaging (T2WI) with fat saturation, multiple b-values of DWI, and dynamic contrast-enhanced (DCE) MRI sequences. A respiratory-triggered single-shot echo planar imaging sequence was employed for DWI, with b-values of 0, 20, 50, 100, 200, 600, 800, 1000, 1200, and 1500 s/mm², respectively. The DWI sequence parameters were: Repetition time (TR)/echo time (TE) = 3000/80; slice thickness = 6 mm; slice gap = 1 mm; matrix = 128 × 90. The total acquisition time for the DWI sequence was approximately 6 min and 19 s. The corresponding parameters for T2WI were: TR/TE = 12630/70 ms; slice thickness = 6 mm; slice gap = 1 mm; matrix = 228 × 224.

MRI image analysis

Images were independently analyzed by two radiologists (B.Z., with 6 years of experience, and H.B.Z with 12 years of experience), utilizing the FuncTool Software implemented in GE Workstation 4.6. The radiologists were blinded to clinical information, pathological results, and each other's findings. To determine the regions of interest (ROI), the radiologists manually drew the ROI on the DWI image with a b-value of 800 s/mm² at the maximum transverse diameter of the hepatic lymph node, avoiding areas containing adjacent vessels and artifacts. T2WI and DCE-MRI images served as references. Additionally, the mean value of parameters obtained from the two observers for each ROI was calculated for further analysis.

The signal intensity (SI) of each ROI was fitted using the following mathematical models, where S(b) is the SI at a particular b value, and S(0) is the SI with b = 0 s/mm²:

(1) ADC was calculated using the mono-exponential model:

$$S(b)/S(0) = \exp(-b \times ADC)$$

(2) Three parameters were calculated using biexponential IVIM model according to the following equation:

$$S(b)/S(0) = f \times \exp(-b \times D^*) + (1-f) \times (-b \times D)$$

D: The true diffusion coefficient; D^* : Pseudo-diffusion coefficient; f: The fraction of pseudo-diffusion.

(3) DDC and α were acquired from SEM using the following mathematical equation:

$$S(b)/S(0) = \exp\{-b \times DDC\}^\alpha$$

DDC: The distributed diffusion coefficient, characterizing the distribution of diffusion rates within a voxel; α : Ranging from 0 to 1, represents intravoxel diffusion heterogeneity.

Surgical technique and clinical information

Hepatic lymph nodes were delineated based on specific criteria, encompassing nodes along the hepatoduodenal ligament, which includes structures like the proper hepatic artery, portal vein, bile duct, and retro-pancreatic head. Nodes along the common hepatic artery and coeliac artery, covering the coeliac, common hepatic, and left gastric arteries, were also considered. Since hepatic lymph nodes were not routinely dissected, only suspected nodes on preoperative imaging and/or intraoperative examination were removed. Hematoxylin and eosin stained specimens of the surgically removed lymph nodes were examined by specialized pathologists, and all pathological results were obtained from final pathological reports.

Clinical information of CRLM patients was collected retrospectively, encompassing age, sex, location (left half colon vs right half colon), T and N stage of the primary tumor, synchronous or metachronous liver metastases, number of liver metastases (single vs multiple), RAS gene status (mutation type vs wild type), treatment response based on RECIST1.1 standard, disappearing lesions (identified when no visible lesion is observed on all imaging sequences after chemotherapy), and levels of carcinoembryonic antigen (CEA) and carbohydrate antigen 19-9 (CA19-9). Serum tumor markers were categorized into two groups: Those within normal limits and those exceeding normal limits, defined as 5 ng/mL for CEA and 40 ng/mL for CA19-9.

Statistical analysis

Continuous variables are presented as mean \pm SD, while categorical variables are expressed as numbers and percentages. To compare characteristics between the two groups, independent-samples *t*/Mann-Whitney or chi-square tests were employed. To identify independent factors associated with hepatic LNM, multivariable logistic regression was conducted using a forward stepwise approach. The diagnostic performance of the predictive model was assessed using the receiver operating characteristic (ROC) curve, and the area under the ROC curve (AUC) with its 95% confidence interval (CI) was calculated. The model's cutoffs were determined using the maximum Youden's method. Sensitivity, specificity, PPV and NPV were also computed to evaluate the model's performance. Inter-observer agreements of quantitative metrics were tested using intraclass correlation coefficients (ICC), with ICC > 0.75 indicating good agreement, 0.40 to 0.75 suggesting moderate agreement, and ≤ 0.40 indicating poor agreement. All statistical analyses were performed using SPSS 25.0 (IBM Corporation, Armonk, NY, United States). A two-sided *P* value less than 0.05 was considered statistically significant, indicating a significant difference or association between variables.

RESULTS

Clinicopathologic characteristics

Among the 97 enrolled patients, 40 patients (41.2%; mean \pm age = 57.53 \pm 9.43 years) exhibited hepatic LNM, while the other 57 patients (58.8%; mean \pm age = 52.91 \pm 10.48 years) did not.

Univariate and multivariate analyses for factors associated with hepatic LNM

In univariate analysis, the short and long axes of the largest lymph node before treatment, short and long axes of the largest lymph node after treatment, pre-treatment D, pre-treatment DDC, post-treatment ADC, post-treatment DDC, and post-treatment α were found to be statistically significant with hepatic LNM ($P < 0.05$).

In multivariate analysis, only pre-treatment DDC (OR < 0.001; $P = 0.002$) and the short axis of the largest lymph node after treatment (OR = 1.509; $P < 0.001$) were identified as independent risk factors for the status of hepatic LNM. The detailed results of the univariate and multivariate analyses are presented in Table 1.

Comparison of parameters from models for prediction hepatic LNM

Table 2 summarizes the results of ROC analysis for quantitative parameters from all three models for predicting hepatic LNM. Pre-DDC had the largest AUC (AUC = 0.770; 95%CI: 0.676-0.865), followed by post-DDC (AUC = 0.739; 95%CI: 0.641-0.838) and post-ADC (AUC = 0.664; 95%CI: 0.553-0.774). The sensitivity, specificity, PPV, NPV, and accuracy of pre-DDC for differentiating malignant and benign hepatic lymph nodes were 85.0%, 59.6%, 59.6%, 85.0%, and 70.1%, respectively, with an optimal cutoff value of 1.92×10^{-3} mm 2 /s.

Furthermore, the short axis of the largest lymph node before and after treatment also exhibited good performance in predicting hepatic LNM. The highest accuracy (77.3%) was achieved at a cutoff value of 10 mm (the best cut off value = 9.5 mm) for the short axis of the largest hepatic lymph node after treatment, which had 52.5% sensitivity and 94.7% specificity for differentiating the status of hepatic lymph nodes.

Development the nomogram for prediction hepatic LNM

The nomogram, incorporating pre-treatment DDC and the short axis of the largest lymph node after treatment, exhibited effective performance in predicting hepatic LNM. The AUC of the nomogram was 0.873 (95%CI: 0.803-0.943) (Figure 1), with sensitivity, specificity, PPV, NPV, and accuracy at 82.5%, 82.5%, 87.0%, 76.7%, and 82.5%, respectively. The nomogram for predicting hepatic LNM is presented in Figure 2.

Interobserver agreement for radiologic parameters

Moderate or good interobserver agreement was achieved for quantitative parameters (ICC range: 0.47-0.83). The ICCs of DDC before and after treatment were 0.52 and 0.81, respectively.

Table 1 Univariate and multivariate analysis of clinical and magnetic resonance imaging factors for prediction of hepatic lymph nodes metastases

| | | Univariate analysis | | Multivariate analysis | | |
|---|-----------------------|-----------------------------|-----------------------------|-----------------------|---------------------|----------------------|
| | | Non-hepatic LNM (n = 57) | hepatic LNM HLN (n = 40) | P value | OR (95%CI) | |
| Gender | Male/female | 44/13 | 27/13 | 0.029 ^a | | |
| Age | | 52.91 ± 10.48 | 57.53 ± 9.43 | 0.054 | | |
| BMI | | 24.63 ± 3.04 | 24.50 ± 3.04 | 0.842 | | |
| Primary location | Right/left-side | 15/42 | 6/34 | 0.944 | | |
| Differentiation | Low to moderate/High | 55/2 | 40/0 | 0.510 | | |
| T stage of primary tumor | T1+2/T3+4 | 3/54 | 4/36 | 0.650 | | |
| N stage of primary tumor | N0/N+ | 9/48 | 5/35 | 0.149 | | |
| Gene | RAS-wild/mutation | 38/19 | 28/12 | 0.729 | | |
| Simultaneous liver metastases | No/Yes | 13/44 | 12/28 | 0.425 | | |
| Distribution | Solitary/Bilateral | 20/37 | 15/25 | 0.808 | | |
| Number of CRLM | ≤ 3/> 3 | 17/40 | 15/25 | 0.429 | | |
| Size (mm) | | 38.25 ± 27.69 | 37.88 ± 22.11 | 0.944 | | |
| RECIST | Response/Non-response | 33/24 | 21/19 | 0.599 | | |
| Disappearing lesion | No/Yes | 46/11 | 34/6 | 0.584 | | |
| pre-CEA | ≤ 5/> 5 ng/mL | 15/42 | 11/29 | 0.897 | | |
| pre-CA199 | ≤ 40/> 40 U/mL | 26/31 | 17/23 | 0.761 | | |
| post-CEA | ≤ 5/> 5 ng/mL | 27/30 | 17/23 | 0.635 | | |
| post-CA199 | ≤ 40/> 40 U/mL | 33/24 | 25/15 | 0.649 | | |
| Short axis of largest lymph node before treatment | mm | 7.39 ± 2.65 | 11.88 ± 5.35 | < 0.001 ^a | | |
| Long axis of largest lymph node before treatment | mm | 14.25 ± 6.41 | 18.28 ± 7.28 | 0.005 ^a | | |
| Pre-ADC | mm ² /s | 1.54 ± 0.35 | 1.49 ± 0.30 | 0.394 | | |
| Pre-D | mm ² /s | 1.21 ± 0.43 | 1.02 ± 0.25 | 0.005 ^a | | |
| Pre-D* | mm ² /s | 3.33 ± 2.37 | 2.70 ± 2.38 | 0.200 | | |
| Pre-f | | 0.49 ± 0.17 | 0.45 ± 0.14 | 0.330 | | |
| Pre-DDC | mm ² /s | 3.21 ± 1.69 | 2.01 ± 0.83 | < 0.001 ^a | < 0.001 | 0.002 ^a |
| Pre-α | | 0.59 ± 0.17 | 0.62 ± 0.16 | 0.363 | | |
| Short axis of largest lymph node after treatment | mm | 6.74 ± 2.13 | 10.43 ± 3.62 | < 0.001 ^a | 1.509 (1.235-1.845) | < 0.001 ^a |
| Long axis of largest lymph node after treatment | mm | 13.46 ± 5.78 | 17.08 ± 6.82 | 0.006 ^a | | |
| Post-ADC | mm ² /s | 1.64 ± 0.32 | 1.45 ± 0.32 | 0.006 ^a | | |
| Post-D | mm ² /s | 1.35 ± 0.86 | 1.24 ± 0.78 | 0.529 | | |
| Post-D* | mm ² /s | 3.69 ± 2.96 | 3.48 ± 3.38 | 0.751 | | |
| Post-f | | 0.51 ± 0.18 | 0.52 ± 0.18 | 0.732 | | |
| Post-DDC | | 3.46 ± 1.48 | 2.37 ± 0.91 | < 0.001 ^a | | |
| Post-α | | 0.61 ± 0.13 | 0.67 ± 0.13 | 0.035 ^a | | |

^aP values that are significantly different between metastatic and non-metastatic HLN group.

HLN: Hemolymph node; OR: Odds ratio; BMI: Body mass indices; CRLM: Colorectal liver metastases; RECIST: Response Evaluation Criteria In Solid Tumors; CEA: Carcinoembryonic antigen; CA19-9: Carbohydrate antigen 19-9; ADC: Apparent diffusion coefficient; CI: Confidence interval; DDC: Distributed diffusion coefficient; LNM: Lymph node metastases; D: True diffusion coefficient; D*: Pseudo-diffusion coefficient; f: The perfusion fraction; α : Intravoxel water diffusion heterogeneity.

Table 2 Diagnostic performance of quantitative parameters and nomogram in predicting hepatic lymph node metastases in colorectal liver metastases patient

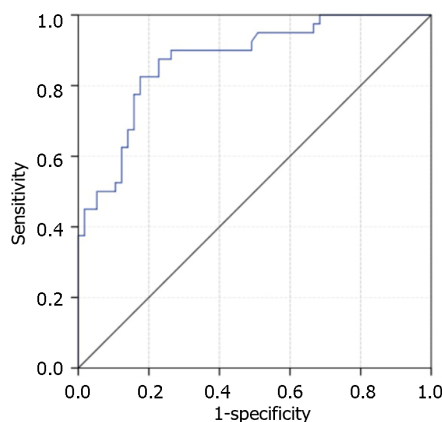
| | AUC | Cut off value | Sensitivity (%) | Specificity (%) | PPV (%) | NPV (%) | Accuracy (%) |
|--|----------------------|---------------|-----------------|-----------------|---------|---------|--------------|
| Pre-ADC | 0.551 (0.436-0.666) | 1.70 | 32.5 | 82.5 | 56.5 | 63.5 | 61.5 |
| Pre-D | 0.648 (0.538-0.758) | 1.15 | 55.0 | 77.2 | 62.9 | 58.1 | 68.0 |
| Pre-D* | 0.592 (0.477-0.707) | 2.51 | 55.0 | 66.7 | 53.7 | 71.0 | 62.1 |
| Pre-f | 0.577 (0.462-0.692) | 3.98 | 70.0 | 47.5 | 48.3 | 64.3 | 56.7 |
| Pre-DDC | 0.770 (0.676-0.865) | 1.92 | 85.0 | 59.6 | 59.6 | 85.0 | 70.1 |
| Pre- α | 0.573 (0.456-0.689) | 0.59 | 62.5 | 59.6 | 52.1 | 69.4 | 60.8 |
| Post-ADC | 0.664 (0.553-0.774) | 1.46 | 75.0 | 52.6 | 52.6 | 75.0 | 61.9 |
| Post-D | 0.581 (0.447-0.681) | 1.21 | 50.0 | 70.2 | 54.1 | 66.7 | 62.1 |
| Post-D* | 0.558 (0.438-0.678) | 1.27 | 85.0 | 33.3 | 47.2 | 76.0 | 54.6 |
| Post-f | 0.521 (0.403-0.638) | 3.98 | 77.5 | 31.6 | 44.3 | 66.7 | 50.5 |
| Post-DDC | 0.739 (0.641-0.838) | 2.26 | 82.5 | 52.5 | 55.0 | 81.1 | 64.9 |
| Post- α | 0.623 (0.509-0.737) | 0.65 | 57.5 | 70.2 | 57.5 | 70.2 | 65.0 |
| Short axis of largest lymph node before treatment (mm) | 0.773 (0.674-0.872) | 12 | 50.0 | 94.7 | 87.0 | 73.0 | 76.3 |
| Short axis of largest lymph node after treatment (mm) | 0.811 (0.724-0.899) | 10 | 52.5 | 94.7 | 38.9 | 74.0 | 77.3 |
| Nomogram | 0.873 (0.803, 0.943) | 1.03 | 82.5 | 82.5 | 87.0 | 76.7 | 82.5 |

AUC: Area under the receiver operating characteristic curve; ADC: Apparent diffusion coefficient; NPV: Negative predictive value; PPV: Positive predictive value; DDC: Distributed diffusion coefficient; D: True diffusion coefficient; D*: Pseudo-diffusion coefficient; f: The perfusion fraction; α : Intravoxel water diffusion heterogeneity.

DISCUSSION

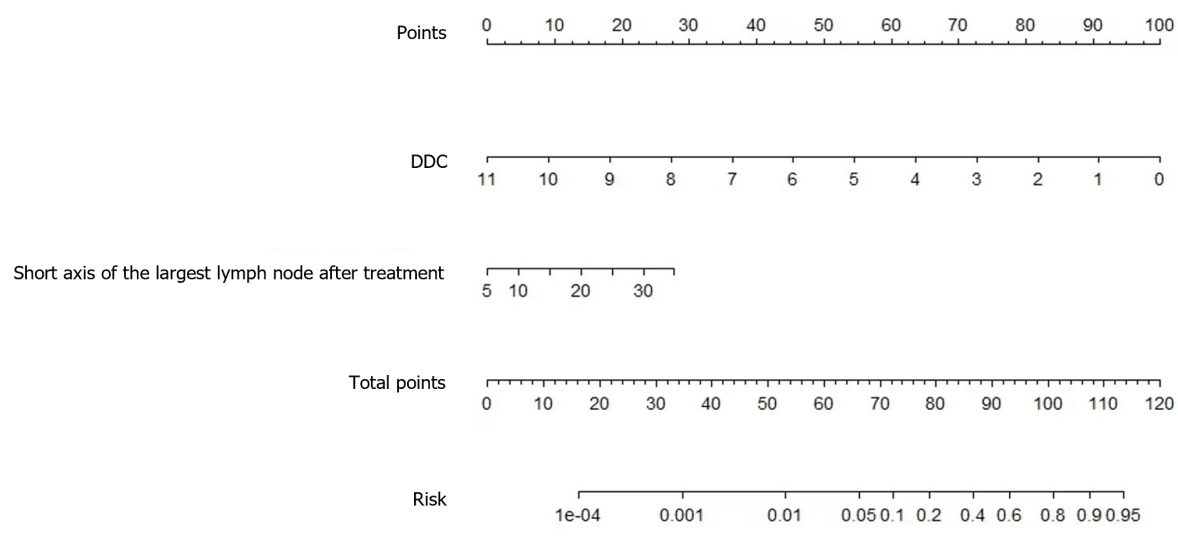
In this study, our goal was to assess the diagnostic potential of DWI parameters using three models to differentiate between benign hepatic lymph nodes and metastatic lymph nodes in patients with initially resectable CRLM. Our findings indicate that the DDC values obtained from the SEM were significantly lower in metastatic lymph nodes compared to non-metastatic lymph nodes, both before and after treatment. Notably, the baseline DDC value exhibited the highest accuracy for preoperative lymph node status diagnosis in CRLM patients, outperforming the accuracy of ADC from the mono-exponential model, as well as D, D*, and f from the IVIM model. Furthermore, there was substantial agreement between two independent readers in assessing DDC, suggesting that DDC, along with the short diameter of the largest lymph node, may serve as a reliable, non-invasive, and promising technique in clinical practice for distinguishing between metastatic and non-metastatic lymph nodes before surgery.

Our results show that the baseline DDC from the SEM demonstrated the highest diagnostic performance in distinguishing metastatic from benign hepatic lymph nodes, followed by post-DDC and post-ADC, although the differences among them were not statistically significant. The DDC value is considered a weighted sum of continuous distributions



DOI: 10.3748/wjg.v30.i4.308 Copyright ©The Author(s) 2024.

Figure 1 The receiver operating characteristic curve of nomogram to predict hepatic lymph node metastases in colorectal liver metastases patients receiving chemotherapy. The area under the curve of the nomogram was 0.873.



DOI: 10.3748/wjg.v30.i4.308 Copyright ©The Author(s) 2024.

Figure 2 Nomogram of model for predicting hepatic lymph node metastases in colorectal liver metastases patients receiving chemotherapy. DDC: Distributed diffusion coefficient.

of ADCs and can offer more information on non-Gaussian distribution. These results can be attributed to increased cellularity, higher nucleus-to-cytoplasm ratios, and more limited extracellular space in malignant lymph nodes, leading to greater intravoxel diffusion heterogeneity[19,20]. Therefore, DDC may have a superior ability to differentiate between benign and malignant liver lesions with minimal overlap compared to ADC calculated from the mono-exponential model, consistent with previous studies on gliomas, ovarian cancer, bladder cancer, and hepatic lesions[21-24]. Additionally, our findings suggest that DDC values calculated from the SEM are more reliable than those from the mono-exponential and IVIM models, aligning with previous studies[25-27].

On the contrary, while quantitative parameters obtained from the IVIM model, except for post-f of benign hepatic lesions, were higher in malignant lymph nodes, the difference was not statistically significant. Several factors may contribute to these results. Firstly, the predictive value of the IVIM model for lymph node status has not been consistently supported in previous literature. For instance, in a study on rectal adenocarcinoma patients, Jia *et al*[28] found that the group with positive lymph nodes exhibited a significantly lower D* value and a higher f value. Conversely, another study on rectal cancer patients showed that the metastatic group had significantly lower D and D* values compared to the nonmetastatic group[29]. Various factors, such as the setting of b-values (especially b-values < 200 s/mm²), TR, and scan techniques, may influence the results of IVIM parameters. Secondly, the heterogeneity of hepatic lesions can impact the quantitative parameters of the IVIM model. Malignant lesions typically demonstrate more heterogeneity in terms of cellularity, vascularity, and perfusion compared to benign lesions. This inherent heterogeneity can lead to variations in the IVIM parameters, making it challenging to differentiate between benign and malignant lesions based solely on IVIM parameters. Additionally, the limited sample size in our study may introduce selection bias.

Our study also revealed that the short diameter of the largest lymph node after treatment was useful in predicting the status of hepatic lymph nodes in CRLM patients. This finding aligns with a previous study indicating tumor size as an independent predictor of lymph node metastases[30]. We identified the optimal diagnostic threshold for the short diameter of lymph nodes as 10 mm, with a sensitivity of 52.5%, specificity of 94.7%, and accuracy of 77.3%. The nomogram, combining DDC and the short diameter of the largest lymph node, can quantitatively evaluate lymph node metastases with enhanced diagnostic efficacy. The nomogram's diagnostic efficiency, with an AUC of 0.873, demonstrated superior performance compared to using either IVIM or SEM alone. Furthermore, the nomogram exhibited improved sensitivity, specificity, and accuracy. These results suggest that the nomogram can effectively prevent unnecessary lymph node dissection in CRLM patients.

The current study has several limitations. Firstly, it was a retrospective, single-center study with a relatively small sample size. Therefore, further studies with a larger sample size and external validation are needed to validate the findings. Secondly, there may be selection bias because we only included patients with clinically suspected lymph node metastasis who underwent surgical resection. This could potentially underestimate the severity of the condition, as most CRLM patients were excluded if they did not have clinically suspicious metastatic lymph nodes. Thirdly, there may be uncertainty regarding the alignment between the lymph node evaluated by the pathologist and the image slices where the DWI parameters were obtained. Additionally, the setting of b-values in DWI remains controversial. While using too many b-values would result in prolonged scan time, further research is required to determine the optimal number and interval of b-values for accurate assessment, considering the trade-off between scan time and accuracy. Lastly, the study did not analyze the relationship between the models and the survival outcome of the patients.

CONCLUSION

In conclusion, our results suggest that a nomogram incorporating the pre-DDC value calculated from SEM-DWI along with the short diameter of the largest lymph node after treatment may have the potential to predict lymph node metastasis noninvasively in CRLM patients after chemotherapy. This nomogram can be used for individualized, noninvasive high-risk assessment and surgical planning for CRLM patients with suspected metastatic hepatic lymph nodes, thereby reducing unnecessary surgical procedures and the occurrence of complications.

ARTICLE HIGHLIGHTS

Research background

More than 50% of patients with colorectal cancer develop colorectal liver metastases (CRLM), and the presence of metastatic hepatic lymph nodes can greatly influence treatment decisions and patient outcomes. Precise preoperative prediction of hepatic lymph node status is beneficial for individualized treatment and reducing complications.

Research motivation

However, there is currently a lack of reliable radiological tools for predicting the presence of metastatic hepatic lymph nodes in CRLM prior to surgery.

Research objectives

The study aimed to assess the predictive ability of different diffusion-weighted imaging (DWI) models (mono-exponential, bi-exponential, and stretched-exponential) in distinguishing between benign and malignant hepatic lymph nodes in CRLM patients who underwent neoadjuvant chemotherapy.

Research methods

A retrospective study was conducted involving 97 CRLM patients with pathologically confirmed hepatic lymph node status who underwent magnetic resonance imaging, including DWI with ten b values before and after chemotherapy. Various parameters, including apparent diffusion coefficient, the true diffusion coefficient, the pseudo-diffusion coefficient, the perfusion fraction, distributed diffusion coefficient (DDC), and α , derived from different DWI models, were measured and compared between positive and negative hepatic lymph node groups. A nomogram was constructed, and the reliability and agreement of the measurements were assessed using appropriate statistical analyses.

Research results

Multivariate analysis revealed that the pre-treatment DDC value and the short diameter of the largest lymph node after treatment were independent predictors of metastatic hepatic lymph nodes. A nomogram combining these factors demonstrated excellent performance in distinguishing between benign and malignant lymph nodes in CRLM patients, with area under the receiver operating characteristic curve of 0.873. Furthermore, parameters from the stretched-exponential model showed substantial repeatability.

Research conclusions

The developed nomogram, incorporating the pre-treatment DDC and the short axis of the largest lymph node, can be

utilized to predict the presence of hepatic lymph node metastases in CRLM patients who undergo chemotherapy prior to surgery. This nomogram was found to be more valuable than quantitative parameters derived from multiple b values of DWI, exhibiting superior diagnostic performance.

Research perspectives

In the future, the nomogram can serve as a preoperative assessment tool for determining the status of hepatic lymph nodes and aiding in the decision-making process for surgical treatment in CRLM patients.

FOOTNOTES

Co-first authors: Hai-Bin Zhu and Bo Zhao.

Author contributions: Zhu HB and Zhao B contributed equally to this work; Zhu HB, Zhao B, Li XT, Zhang XY and Sun YS designed the research study; Zhu HB, Zhao B, Li XT, Zhang XY and Sun YS performed the research; Li XT and Yao Q contributed new reagents and analytic tools; Zhu HB, Zhao B, Li XT and Yao Q analyzed the data and wrote the manuscript; All authors have read and approve the final manuscript.

Supported by Beijing Hospitals Authority Youth Program, No. QML20231103; Beijing Hospitals Authority Ascent Plan, No. DFL20191103; and National Key R&D Program of China, No. 2023YFC3402805.

Institutional review board statement: This study was conducted in accordance with the regulations and guidelines established by the Medical Ethics Committee (IRB) of Beijing Cancer Hospital. All studies involving human subjects were conducted with IRB approval.

Informed consent statement: Informed consent was waived due to the retrospective study.

Conflict-of-interest statement: The authors declared no conflicts of interest.

Data sharing statement: No additional data are available.

Open-Access: This article is an open-access article that was selected by an in-house editor and fully peer-reviewed by external reviewers. It is distributed in accordance with the Creative Commons Attribution NonCommercial (CC BY-NC 4.0) license, which permits others to distribute, remix, adapt, build upon this work non-commercially, and license their derivative works on different terms, provided the original work is properly cited and the use is non-commercial. See: <https://creativecommons.org/Licenses/by-nc/4.0/>

Country/Territory of origin: China

ORCID number: Hai-Bin Zhu [0000-0002-6239-6333](#); Xiao-Ting Li [0000-0003-2758-3843](#); Xiao-Yan Zhang [0000-0003-2700-7627](#); Ying-Shi Sun [0000-0001-9424-1910](#).

S-Editor: Fan JR

L-Editor: A

P-Editor: Chen YX

REFERENCES

- 1 Ferlay J, Soerjomataram I, Dikshit R, Eser S, Mathers C, Rebelo M, Parkin DM, Forman D, Bray F. Cancer incidence and mortality worldwide: sources, methods and major patterns in GLOBOCAN 2012. *Int J Cancer* 2015; **136**: E359-E386 [PMID: [25220842](#) DOI: [10.1002/ijc.29210](#)]
- 2 Nieuwenhuizen S, Puijk RS, van den Bemd B, Aldrighetti L, Arntz M, van den Boezem PB, Bruynzeel AME, Burgmans MC, de Cobelli F, Coolsen MME, Dejong CHC, Derkx S, Diederik A, van Duijvendijk P, Eker HH, Engelsman AF, Erdmann JI, Fütterer JJ, Geboers B, Groot G, Haasbeek CJA, Janssen JJ, de Jong KP, Kater GM, Kazemier G, Kruimier JWH, Leclercq WKG, van der Leij C, Manusama ER, Meier MAJ, van der Meij BB, Melenhorst MCAM, Nielsen K, Nijkamp MW, Potters FH, Prevoo W, Rietema FJ, Ruuris AH, Ruiter SJS, Schouten EAC, Serafino GP, Sietses C, Swijnenburg RJ, Timmer FEF, Versteeg KS, Vink T, de Vries JJJ, de Wilt JHW, Zonderhuis BM, Scheffer HJ, van den Tol PMP, Meijerink MR. Resectability and Ablatability Criteria for the Treatment of Liver Only Colorectal Metastases: Multidisciplinary Consensus Document from the COLLISION Trial Group. *Cancers (Basel)* 2020; **12** [PMID: [32635230](#) DOI: [10.3390/cancers12071779](#)]
- 3 Morris VK, Kennedy EB, Baxter NN, Benson AB 3rd, Cercek A, Cho M, Ciombor KK, Cremolini C, Davis A, Deming DA, Fakih MG, Gholami S, Hong TS, Jaiyesimi I, Klute K, Lieu C, Sanoff H, Strickler JH, White S, Willis JA, Eng C. Treatment of Metastatic Colorectal Cancer: ASCO Guideline. *J Clin Oncol* 2023; **41**: 678-700 [PMID: [36252154](#) DOI: [10.1200/JCO.22.01690](#)]
- 4 Liu W, Yan XL, Wang K, Bao Q, Sun Y, Xing BC. The outcome of liver resection and lymphadenectomy for hilar lymph node involvement in colorectal cancer liver metastases. *Int J Colorectal Dis* 2014; **29**: 737-745 [PMID: [24743847](#) DOI: [10.1007/s00384-014-1863-5](#)]
- 5 Elias D, Saric J, Jaeck D, Arnaud JP, Gayet B, Rivoire M, Lorimier G, Carles J, Lasser P. Prospective study of microscopic lymph node involvement of the hepatic pedicle during curative hepatectomy for colorectal metastases. *Br J Surg* 1996; **83**: 942-945 [PMID: [8813780](#) DOI: [10.1002/bjs.1800830717](#)]
- 6 Ercolani G, Grazi GL, Ravaioli M, Grigioni WF, Cescon M, Gardini A, Del Gaudio M, Cavallari A. The role of lymphadenectomy for liver tumors: further considerations on the appropriateness of treatment strategy. *Ann Surg* 2004; **239**: 202-209 [PMID: [14745328](#) DOI: [10.1097/00000653-200403000-00004](#)]

- 10.1097/01.sla.0000109154.00020.e0]
- 7** **Ishizuka D**, Shirai Y, Hatakeyama K. Ischemic biliary stricture due to lymph node dissection in the hepatoduodenal ligament. *Hepatogastroenterology* 1998; **45**: 2048-2050 [PMID: 9951863]
- 8** **Grobmyer SR**, Wang L, Gonon M, Fong Y, Klimstra D, D'Angelica M, DeMatteo RP, Schwartz L, Blumgart LH, Jarnagin WR. Perihepatic lymph node assessment in patients undergoing partial hepatectomy for malignancy. *Ann Surg* 2006; **244**: 260-264 [PMID: 16858189 DOI: 10.1097/01.sla.0000217606.59625.9d]
- 9** **Rau C**, Blanc B, Ronot M, Dokmak S, Aussilhou B, Faivre S, Vilgrain V, Paradis V, Belghiti J. Neither preoperative computed tomography nor intra-operative examination can predict metastatic lymph node in the hepatic pedicle in patients with colorectal liver metastasis. *Ann Surg Oncol* 2012; **19**: 163-168 [PMID: 21837526 DOI: 10.1245/s10434-011-1994-7]
- 10** **Ko CC**, Yeh LR, Kuo YT, Chen JH. Imaging biomarkers for evaluating tumor response: RECIST and beyond. *Biomark Res* 2021; **9**: 52 [PMID: 34215324 DOI: 10.1186/s40364-021-00306-8]
- 11** **Messina C**, Bignone R, Bruno A, Bruno F, Calandri M, Caruso D, Coppolino P, Robertis R, Gentili F, Grazzini I, Natella R, Scalise P, Barile A, Grassi R, Albano D. Diffusion-Weighted Imaging in Oncology: An Update. *Cancers (Basel)* 2020; **12** [PMID: 32521645 DOI: 10.3390/cancers12061493]
- 12** **Bonekamp S**, Corona-Villalobos CP, Kamel IR. Oncologic applications of diffusion-weighted MRI in the body. *J Magn Reson Imaging* 2012; **35**: 257-279 [PMID: 22271274 DOI: 10.1002/jmri.22786]
- 13** **Sumi M**, Sakihama N, Sumi T, Morikawa M, Uetani M, Kabasawa H, Shigeno K, Hayashi K, Takahashi H, Nakamura T. Discrimination of metastatic cervical lymph nodes with diffusion-weighted MR imaging in patients with head and neck cancer. *AJNR Am J Neuroradiol* 2003; **24**: 1627-1634 [PMID: 13679283]
- 14** **Abdel Razek AA**, Soliman NY, Elkhamary S, Alsharaway MK, Tawfik A. Role of diffusion-weighted MR imaging in cervical lymphadenopathy. *Eur Radiol* 2006; **16**: 1468-1477 [PMID: 16557366 DOI: 10.1007/s00330-005-0133-x]
- 15** **Eiber M**, Beer AJ, Holzapfel K, Tauber R, Ganter C, Weirich G, Krause BJ, Rummeny EJ, Gaa J. Preliminary results for characterization of pelvic lymph nodes in patients with prostate cancer by diffusion-weighted MR-imaging. *Invest Radiol* 2010; **45**: 15-23 [PMID: 1996762 DOI: 10.1097/RLL.0b013e3181bbdc2f]
- 16** **Zhou XJ**, Gao Q, Abdullah O, Magin RL. Studies of anomalous diffusion in the human brain using fractional order calculus. *Magn Reson Med* 2010; **63**: 562-569 [PMID: 20187164 DOI: 10.1002/mrm.22285]
- 17** **Ai Z**, Han Q, Huang Z, Wu J, Xiang Z. The value of multiparametric histogram features based on intravoxel incoherent motion diffusion-weighted imaging (IVIM-DWI) for the differential diagnosis of liver lesions. *Ann Transl Med* 2020; **8**: 1128 [PMID: 33240977 DOI: 10.21037/atm-20-5109]
- 18** **Bennett KM**, Schmaind KM, Bennett RT, Rowe DB, Lu H, Hyde JS. Characterization of continuously distributed cortical water diffusion rates with a stretched-exponential model. *Magn Reson Med* 2003; **50**: 727-734 [PMID: 14523958 DOI: 10.1002/mrm.10581]
- 19** **Liu C**, Wang K, Li X, Zhang J, Ding J, Spuhler K, Duong T, Liang C, Huang C. Breast lesion characterization using whole-lesion histogram analysis with stretched-exponential diffusion model. *J Magn Reson Imaging* 2018; **47**: 1701-1710 [PMID: 29165847 DOI: 10.1002/jmri.25904]
- 20** **Seo N**, Chung YE, Park YN, Kim E, Hwang J, Kim MJ. Liver fibrosis: stretched exponential model outperforms mono-exponential and bi-exponential models of diffusion-weighted MRI. *Eur Radiol* 2018; **28**: 2812-2822 [PMID: 29404771 DOI: 10.1007/s00330-017-5292-z]
- 21** **Bai Y**, Lin Y, Tian J, Shi D, Cheng J, Haacke EM, Hong X, Ma B, Zhou J, Wang M. Grading of Gliomas by Using Monoexponential, Biexponential, and Stretched Exponential Diffusion-weighted MR Imaging and Diffusion Kurtosis MR Imaging. *Radiology* 2016; **278**: 496-504 [PMID: 26230975 DOI: 10.1148/radiol.2015142173]
- 22** **Wang F**, Wang Y, Zhou Y, Liu C, Xie L, Zhou Z, Liang D, Shen Y, Yao Z, Liu J. Comparison between types I and II epithelial ovarian cancer using histogram analysis of monoexponential, biexponential, and stretched-exponential diffusion models. *J Magn Reson Imaging* 2017; **46**: 1797-1809 [PMID: 28379611 DOI: 10.1002/jmri.25722]
- 23** **Wang Y**, Hu D, Yu H, Shen Y, Tang H, Kamel IR, Li Z. Comparison of the Diagnostic Value of Monoexponential, Biexponential, and Stretched Exponential Diffusion-weighted MRI in Differentiating Tumor Stage and Histological Grade of Bladder Cancer. *Acad Radiol* 2019; **26**: 239-246 [PMID: 29753491 DOI: 10.1016/j.acra.2018.04.016]
- 24** **Hu Y**, Tang H, Li H, Li A, Li J, Hu D, Li Z, Kamel IR. Assessment of different mathematical models for diffusion-weighted imaging as quantitative biomarkers for differentiating benign from malignant solid hepatic lesions. *Cancer Med* 2018; **7**: 3501-3509 [PMID: 29733515 DOI: 10.1002/cam4.1535]
- 25** **Li H**, Liang L, Li A, Hu Y, Hu D, Li Z, Kamel IR. Monoexponential, biexponential, and stretched exponential diffusion-weighted imaging models: Quantitative biomarkers for differentiating renal clear cell carcinoma and minimal fat angiomyolipoma. *J Magn Reson Imaging* 2017; **46**: 240-247 [PMID: 27859853 DOI: 10.1002/jmri.25524]
- 26** **Kim HC**, Seo N, Chung YE, Park MS, Choi JY, Kim MJ. Characterization of focal liver lesions using the stretched exponential model: comparison with monoexponential and biexponential diffusion-weighted magnetic resonance imaging. *Eur Radiol* 2019; **29**: 5111-5120 [PMID: 30796578 DOI: 10.1007/s00330-019-06048-4]
- 27** **Jerome NP**, Miyazaki K, Collins DJ, Orton MR, d'Arcy JA, Wallace T, Moreno L, Pearson AD, Marshall LV, Carceller F, Leach MO, Zacharoulis S, Koh DM. Repeatability of derived parameters from histograms following non-Gaussian diffusion modelling of diffusion-weighted imaging in a paediatric oncological cohort. *Eur Radiol* 2017; **27**: 345-353 [PMID: 27003140 DOI: 10.1007/s00330-016-4318-2]
- 28** **Jia H**, Jiang X, Zhang K, Shang J, Zhang Y, Fang X, Gao F, Li N, Dong J. A Nomogram of Combining IVIM-DWI and MRI Radiomics From the Primary Lesion of Rectal Adenocarcinoma to Assess Nonenlarged Lymph Node Metastasis Preoperatively. *J Magn Reson Imaging* 2022; **56**: 658-667 [PMID: 35090079 DOI: 10.1002/jmri.28068]
- 29** **Wang C**, Yu J, Lu M, Li Y, Shi H, Xu Q. Diagnostic Efficiency of Diffusion Sequences and a Clinical Nomogram for Detecting Lymph Node Metastases from Rectal Cancer. *Acad Radiol* 2022; **29**: 1287-1295 [PMID: 34802905 DOI: 10.1016/j.acra.2021.10.009]
- 30** **Zhu HB**, Xu D, Sun XF, Li XT, Zhang XY, Wang K, Xing BC, Sun YS. Prediction of hepatic lymph node metastases based on magnetic resonance imaging before and after preoperative chemotherapy in patients with colorectal liver metastases underwent surgical resection. *Cancer Imaging* 2023; **23**: 18 [PMID: 36810192 DOI: 10.1186/s40644-023-00529-y]



Published by **Baishideng Publishing Group Inc**
7041 Koll Center Parkway, Suite 160, Pleasanton, CA 94566, USA

Telephone: +1-925-3991568

E-mail: office@baishideng.com

Help Desk: <https://www.f6publishing.com/helpdesk>

<https://www.wjnet.com>

